Bioconjugate Chemistry

Article

pubs.acs.org/bc

Statistical Modeling of the Drug Load Distribution on Trastuzumab Emtansine (Kadcyla), a Lysine-Linked Antibody Drug Conjugate

Michael T. Kim,*[,†] Yan Chen,[†] Joseph Marhoul,[‡] and Fred Jacobson[†]

[†]Departments of Protein Analytical Chemistry and [‡]Biostatistics Genentech, Inc, South San Francisco, California 94080 United States

ABSTRACT: Trastuzumab emtansine (Kadcyla) is a recently approved antibody−drug conjugate produced by attachment of the anti-tubulin drug, DM1, to lysine amines via the SMCC linker. The resulting product exhibits a drug load distribution from 0 to 8 drugs per antibody that can be quantified using mass spectrometry. Different statistical models were tested against the experimental data derived from samples produced during process characterization studies to determine best fit. The Poisson distribution gives the best correlation for samples manufactured using the target process conditions (yielding the target average drug to antibody ratio (DAR) of 3.5) as well as those produced under conditions that exceed the allowed manufacturing ranges and yield products with average DAR values that are significantly different from the target (i.e., ≤3.0 or ≥4.0). The Poisson distribution establishes a link between average DAR values and drug load distributions, implying that measurement and control of the former (i.e., via a simple UV spectrophotometric method) could be used to indirectly control the latter in trastuzumab emtansine.

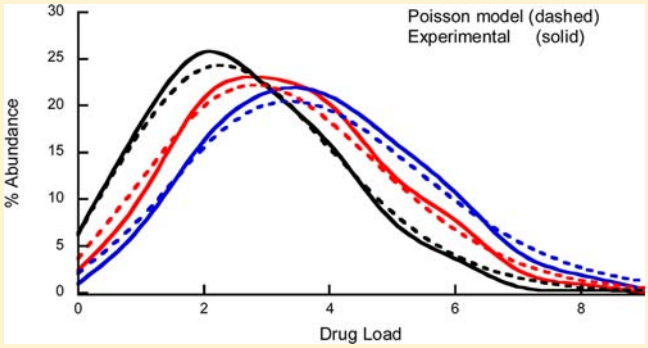

INTRODUCTION

Monoclonal antibodies (mAb) coupled to potent cytotoxic chemotherapy drugs (antibody−drug conjugates or ADCs)[1,2] are currently being developed and evaluated for a variety of indications including CD22+ non-Hodgkin's lymphoma and HER2+ metastatic breast cancer.[3,4] The 2011 approval of Adcetris, an ADC targeting $CD30^+$ Hodgkin's lymphoma, and the 2013 approval of Kadcyla, an ADC targeting $HER2^+$ breast cancer, have confirmed the clinical benefit that these therapeutic products can deliver.[5] ADCs combine the biological specificity of an mAb with the high potency of a small molecule drug to create a single targeted agent with greater efficacy and lower systemic toxicity than traditional chemotherapy.

For most ADCs in clinical development, the covalent attachment of drugs is either through the lysine amines of the antibody or through interchain cysteine thiols. One of the most important quality attributes of an ADC is the average drug to antibody ratio (DAR), because this determines the amount of "payload" that can be delivered to the tumor cell and can directly affect both safety and efficacy.[6] Relative to antibodies engineered with specific sites of attachment,[7] conjugation reactions on native mAbs result in populations of ADC molecules that are more heterogeneous with respect to the loading of cytotoxic drug species.[8−12] The resulting distribution of drug-linked forms is also an important ADC characteristic because different drug-loaded forms may have different pharmacokinetic and/or toxicological properties.[13] Hamblett et al. described in vitro studies with purified fractions of cysteine-linked MMAE conjugates, demonstrating that cell-based potency increased with increasing drug load (IC_{50} values drug load 8 < drug load 4 < drug load 2). In vivo, the higher drug-load species cleared more rapidly and were more likely to induce toxicity.[13] This phenomenon may be related to the specific sites that are conjugated in the higher drug-loaded species, to structural changes associated with the high drug load, or to other physicochemical characteristics of the conjugated drug. Although the impact of drug load distribution on PK of lysine-linked conjugates has not been similarly characterized due to the difficulty of isolating conjugate pools with a narrow DAR range, it is still important to understand the relationships between the conjugation process, the average DAR, and the distribution of drug-loaded forms. If a robust, well-defined relationship can be identified linking average DAR to the drug-load distribution, it may be possible to use a simple UV-spectrophotometric method as a control for both quality attributes.

For ADCs where the drug-linker and antibody have different absorbance maxima, average DAR can be determined using UV/vis spectroscopic analysis.[6] Determining the drug load distribution, however, can be considerably more challenging, especially for lysine-linked conjugates. While the drug load distribution of cysteine-linked conjugates can typically be determined chromatographically,[6] species that differ in the number of drugs attached through lysine residues are not easily separated by chromatography due to their high degree of heterogeneity. Imaged capillary isoelectric focusing (iCIEF) can separate the different drug load species of lysine-linked conjugates, but quantification is confounded by charge

Received: January 6, 2014
Revised: May 21, 2014
Published: May 29, 2014

dx.doi.org/10.1021/bc5000109 | *Bioconjugate Chem.* 2014, 25, 1223−1232

associated variants of the antibody intermediate, cross-linking (if present), and potential differences in UV response of the differentially drug-loaded forms. Several published reports have described the use of mass spectrometry (MS) to characterize the distribution of lysine-linked conjugates and ADCs.[9,10,14,15] In these studies, Fc-Alexa Fluor 350, trastuzumab emtansine (T-DM1), anti-CD22-MCC-DM1 and huN901-DM1 exhibit smooth, unimodal load distributions. The only published exception is gemtuzumab ozogamicin (Mylotarg), which was first approved for treatment of $CD33^+$ acute myeloid leukemia in 2000 but withdrawn from the market in 2010. It was also a lysine conjugate with an average DAR of ~3 drugs per antibody. Kunz showed that it consisted of ~50% unconjugated antibody (referred to as low conjugate fraction) with the remainder being a mixture averaging ~6 drugs/mAb.[16] It was also reported that changing conjugation conditions can significantly reduce the level of unconjugated mAb (to ~10%). To date, the factors responsible for this bimodal distribution are not well understood.

T-DM1 (trastuzumab emtansine) combines the anti-HER2 antibody, trastuzumab (Herceptin) with the cytotoxic microtubule-inhibiting, maytansine derivative, DM1, and is currently being developed for the treatment of HER2+ breast cancer.[4,17] This conjugate was approved by the FDA in early 2013 under the name Kadcyla. Figure 1 illustrates the two-step conjugation process for T-DM1. In the first step, the antibody is reacted with the NHS-activated ester of the heterobifunctional linker, SMCC, to produce the linker-modified intermediate. DM1, which contains a free thiol group, is added in the second step and reacts with the maleimide to produce the thioether-linked drug conjugate. When run at the target process conditions, a consistent distribution of DM1-conjugated forms with a reproducible average DAR of 3.5 drugs per antibody (as determined by UV spectroscopy) is produced. Mass spectrometric analysis (Figure 2) demonstrates that T-DM1 is composed of a mixture of species with different individual DARs (ranging from 0 to 8). Integration of the deconvoluted MS profiles, followed by weight averaging, gives an MS-derived DAR that correlates well to the average DAR measured by UV spectroscopy (Figure 3). A similar comparison between DAR measured using UV spectroscopy and mass spectrometry for a lysine conjugate was recently published by Boylan et al.[15]

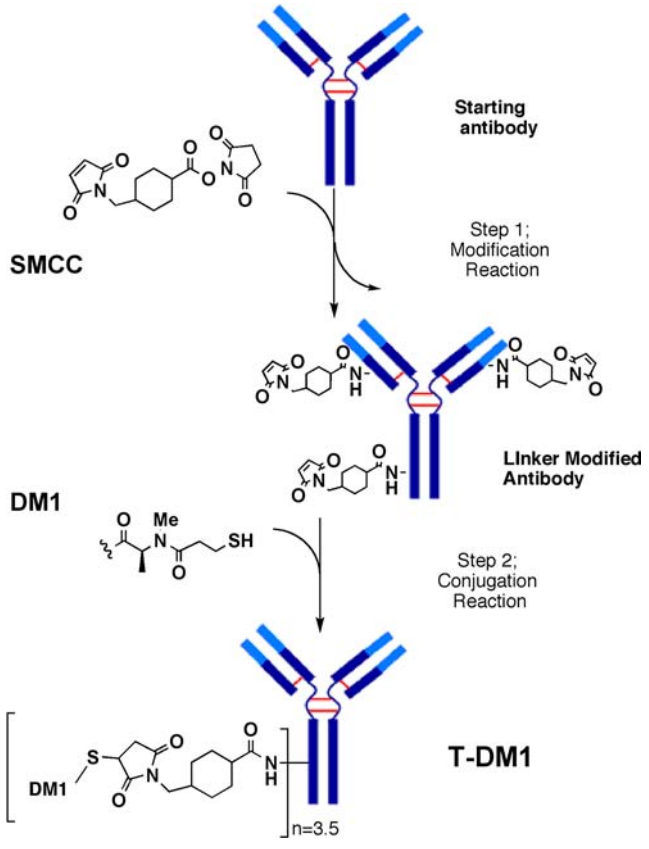

Figure 1. Schematic of T-DM1 conjugation: modification of lysines on trastuzumab with SMCC linker and subsequent reaction with the sulfhydryl of the DM1 drug. Figure adapted from Wakankar et al.[17]

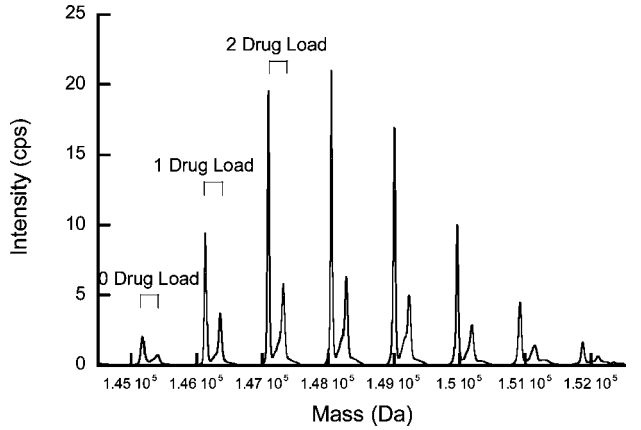

Figure 2. Deconvoluted intact mass graph of T-DM1 reference sample from LC-MS.

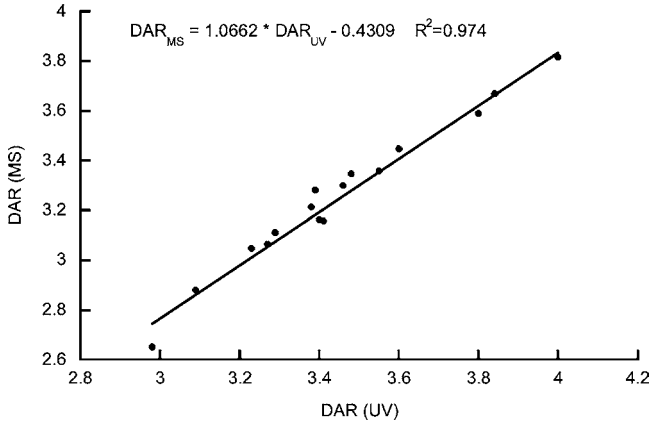

Figure 3. Comparison of average DAR determined via UV-spectroscopy and via mass spectrometry.

In order to develop an understanding of how the distribution of drug on the antibody varies as a function of average DAR, T-DM1 samples with average DAR values ranging from 2.58 to 4.00 were analyzed by ESI-TOF MS. These samples were derived from small-scale multivariate process characterization studies, where variable process conditions were used to perturb product quality attributes. The relative abundances of the heterogeneous drug load species in these samples were determined using intact LC-MS. A numerical analysis of the mass spectrometric data yielded two suitable discrete models that relate drug load distribution to average DAR. A strictly numerical analysis as a first pass screen allowed for an unbiased

dx.doi.org/10.1021/bc5000109 | Bioconjugate Chem. 2014, 25, 1223−1232

consideration of all standard discrete models and revealed how selective, or promiscuous, this data set was when fitting models. The two models resulting from the numerical analysis were then evaluated to determine how well they agreed with the understood chemistry of the conjugation process.

Using this approach, a relationship between average DAR and drug load distribution has been established which is described by the Poisson distribution. While it has been previously suggested that lysine-conjugated reactions yield a Poisson distribution of drug-loaded forms, there was limited published data to corroborate this claim with significant statistical power.[18−20] In this study, we examine a substantial set of data ($n > 16$) generated from the multivariate process characterization studies and perform hold-out cross-validation on the data set to assess the accuracy of the Poisson model. We demonstrate that the manufacture of T-DM1 yields conjugates with a Poisson distribution for all conditions allowed by the manufacturing process as well as for conditions that exceed these limits.

RESULTS AND DISCUSSION

Intact Mass Analysis Using LC/MS. In the manufacture of trastuzumab emtansine, outlined in Figure 1, lysines on trastuzumab are first modified by reaction with SMCC linkers to form an intermediate product. The subsequent conjugation to DM1 drugs via a Michael addition reaction yields the final product. As mentioned previously, this process results in a product characterized by a distribution of differentially drug-loaded species. Intact LC-MS analysis was used to determine the drug load distribution as shown in the deconvoluted mass spectrum of a typical sample (Figure 2). The masses in the series are separated by 958 Da, or the mass of one DM1 drug and one MCC linker, and this corresponds to the drug load species, i.e., 0-drug, 1-drug, 2-drug, etc. (the relative mass error was less than 10 ppm). A second, less abundant series of peaks can be observed separated from the primary peak series by an offset of 219 Da, which are attributable to linkers that have modified the antibody but do not contain conjugated DM1 due to a side-reaction. For the sake of quantification and model testing, all peaks with the same drug load were lumped together, i.e., 2-drug, 2-drug+1-linker, 2-drug+2-linker, to calculate the relative abundance of that drug load in a given sample.

Comparison of the mass spectra from samples produced using the target and nontarget process conditions showed drug load profiles that were both smooth and unimodal. As expected, for samples with higher or lower average DAR (by UV), the drug load distributions are skewed to the higher or lower mass ranges, respectively, indicating that the centroid, or weighted average, of the distribution correlated with the average DAR. The MS data from each sample was evaluated to identify a model that could accurately link the drug load distributions to the average DAR as determined by UV spectroscopy (DAR_{UV}).

Evaluation of Standard Statistical Models. Five standard discrete statistical models were fitted and tested against the "training" data set. Three out of the five models tested did not warrant further consideration for different reasons. The geometric distribution is one that would result in a strictly decreasing fraction as a function of drug load, and so it did not resemble the experimentally observed distributions. When optimizing the parameters of the negative binomial distribution, one of the parameters increased without bound and the distribution converged to a Poisson distribution. Similarly, when optimizing the parameters of the hypergeometric distribution, its parameters increased without bound and the distribution converged to a binomial distribution. Therefore, the detailed model analysis focused only on the binomial and Poisson models.

Fitting Data with the Poisson Model. Based on a visual inspection of the MS distributions, the most likely statistical model was based on the Poisson distribution. The Poisson distribution, is mathematically defined as

$$P(x) = \frac{\lambda^x}{x!}e^{-\lambda} \tag{1}$$

where $P(x)$ is the probability of an event occurring x times and λ is the average number of times for that event to occur. In the context of trastuzumab emtansine's structure, it was expected that $P(x)$ would correspond to the fraction of the sample having x number of DM1 drugs and average DAR_{UV} would equal λ, i.e., the mean of the drug load distribution (% Abundance referenced in the figures is equivalent to $100{\cdot}P(x)$). Substituting DAR_{UV} determined by UV spectroscopy directly for λ in eq 1 and calculating $P(x)$ for each $x = 0$ through 8, the model reproduced the general shape of the experimental drug load distributions by MS, but the apexes from the model distributions were systematically offset compared to the experimental distributions (results not shown).

In order to refine the basic Poisson model, we observed a slight discrepancy in DAR depending on how it was determined. Figure 3 shows that the average DAR_{UV}, which was calculated from UV measurements (as described in the Computational Methods section), and the DAR calculated from the intact LC/MS data (DAR_{MS}) are slightly different (by ~0.2 drugs per antibody) but highly correlated ($R^2 = 0.974$). A similar difference between UV and MS derived conjugation ratio was noted by Boylan et al. for their characterization of an Fc-Alexa Fluor dye conjugate.[15] This difference might be explained by an unequal response in the mass spectrometer between the different drug load species, i.e., reduced ionization of more highly drug-loaded species with less positive charge.[21] An alternative explanation, that the UV-DAR is affected by changes to the extinction coefficient of the drug due to the local environment,[22] is less likely due to the multiplicity of surface accessible lysine linkage sites occupied in T-DM1 leading to less impact from a specific drug/protein interaction. Using the data set and linear equation shown in Figure 3 (eq 2a), the UV determined DAR values (DAR_{UV}) were converted to LC/MS equivalent DAR (DAR_{calc}) values and substituted into the Poisson model:

$$DAR_{calc} = 1.0662{\cdot}DAR_{UV} - 0.4309 \tag{2a}$$

$$P(x) = \frac{(DAR_{calc})^x}{x!}e^{-DAR_{calc}} \tag{2b}$$

A parallel, purely statistical analysis that fit the 16 experimental data sets to the Poisson model using a linear function of the DAR_{UV} values, while minimizing the total variation distance, resulted in a very similar final model ($DAR_{calc} = 1.0999 \times DAR_{UV} - 0.4984$). The model from eq 2b (generated using the MS derived DAR_{calc}) predicted drug load distributions comparable to the experimental data for three samples with low, mid, and high DAR (Figure 5). Extending the analysis for all 16 "training" samples showed that the model tracked the individual drug load species well (0 to 8 DM1 drugs, Figure 6).

dx.doi.org/10.1021/bc5000109 | Bioconjugate Chem. 2014, 25, 1223−1232

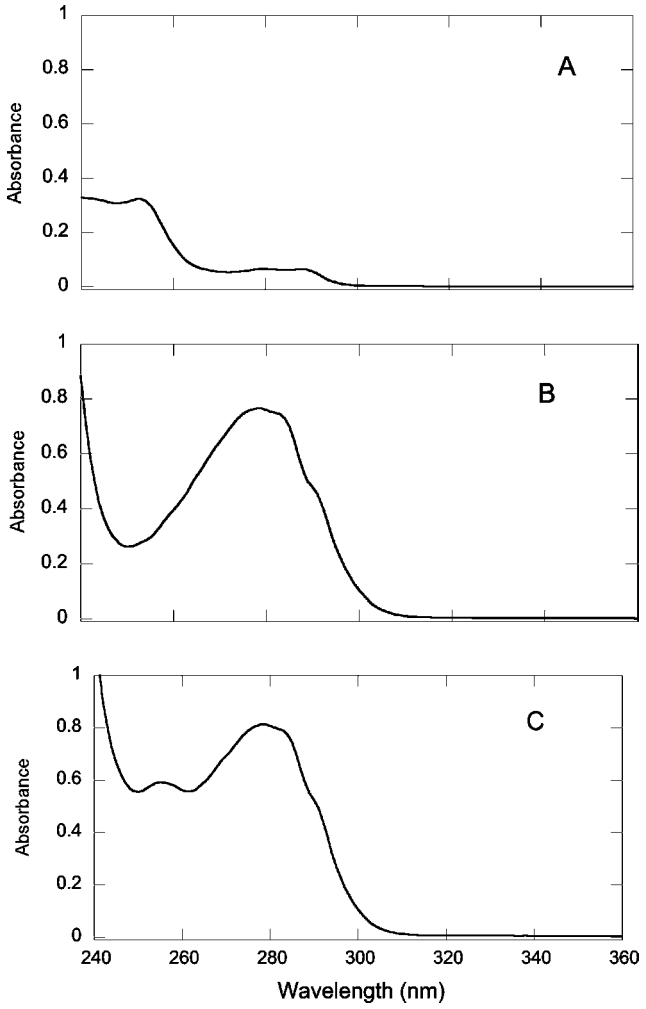

Figure 4. UV spectroscopy of DM1, trastuzumab, and T-DM1. Panel A = DM1 in acetonitrile at 0.012 mg/mL. Panel B = trastuzumab at 0.5 mg/mL. Panel C = T-DM1, with an average DAR of 3.5, at 0.5 mg/mL.

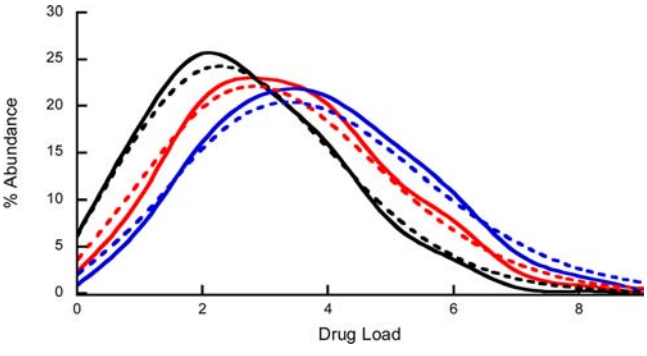

Figure 5. Comparison of Poisson modeled (dashed lines) and experimentally determined (solid lines) drug load distributions for three representative DAR_{UV} = 2.98 (black), 3.48 (red), and 4.00 (blue). Experimentally determined drug load distributions are fitted from discrete data points.

The most rigorous test of a statistical model is to assess its performance against novel data sets not included in the model generation. A related alternative is to use cross-validation. The advantage of a cross-validation procedure is that it establishes mutual exclusivity between samples that are used to train (i.e., derive) and to validate a model, without the need to produce and analyze additional samples. As a result, cross-validation statistics avoid a common pitfall regarding overfitting bias and overly optimistic accuracy values, while at the same time remaining economical and practical. The cross-validation procedure showed that even the worst-fitting model—out of all the possible model permutations from "training" data sets—had a maximum error limited to 3.4% between the observed and predicted abundance of any specific drug load species.

Upon closer examination, Figure 6 revealed that the largest discrepancies between the Poisson model and experimental data are from the 0, 1, 3, and 4 drug loads. Since the 3 and 4 drug loads are the most abundant, the model appears less accurate near the target average DAR. While the exact mechanism for this discrepancy is unclear at this time, it could be related to ion suppression. Because the 0 to 5 drug load species elute at similar retention times on LC/MS (data not shown), the signal for the abundant 3 and 4 drug loads might be enhanced at the expense of the signal for the 0 and 1 drug loads. Meanwhile, the other low abundant 6, 7, and 8 drug load species, which do not coelute with the abundant 3 and 4 drug loads, remain largely unaffected.

Fitting Data with the Binomial Model. A close relative to the Poisson distribution, the binomial distribution, is mathematically defined as

$$B(x) = \frac{N!}{x!(N-x)!}p^x(1-p)^{N-x} \tag{3}$$

where $B(x)$ is the probability of an event occurring x times given N number of trials and p probability that an event will occur in a trial. In the context of trastuzumab emtansine, it was expected that $B(x)$ would correspond to the fraction of the sample having x number of DM1 drugs and the parameters p and N would equal the probability of conjugating any available lysine and the total number of available lysines, respectively.

In order to enable fitting the binomial model to our experimental data, eq 3 was rewritten to include a parameter that corresponds to DAR. The average DAR (λ) can be expressed using the following relationship between N (number of available sites) and p (average probability of modification at any available site):

$$\lambda = N \cdot p \tag{4}$$

After rearrangement to express p as λ/N and substitution into eq 3, the binomial model can be expressed as a function of average DAR (λ) and N.

The statistical analysis to find the optimal binomial model fit for our data was more complicated than with the Poisson model because of the need to optimize two parameters instead of one. To reduce the optimization complexity from a two-dimensional to a one-dimensional problem, we generated a separate binomial model for each possible integral value of N (up to N = 92 sites), thus decoupling N from the model fitting process. Each binomial model could then be fitted to the drug load distribution data in much the same way as the Poisson model was fitted, as a function of average DAR. The iteration (N = 17 sites) with the lowest discrepancy between modeled and experimental drug load distributions was chosen as the final binomial model

$$p_{calc} = \frac{1.0602 \cdot DAR_{UV} - 0.4275}{17} \tag{5a}$$

dx.doi.org/10.1021/bc5000109 | Bioconjugate Chem. 2014, 25, 1223−1232

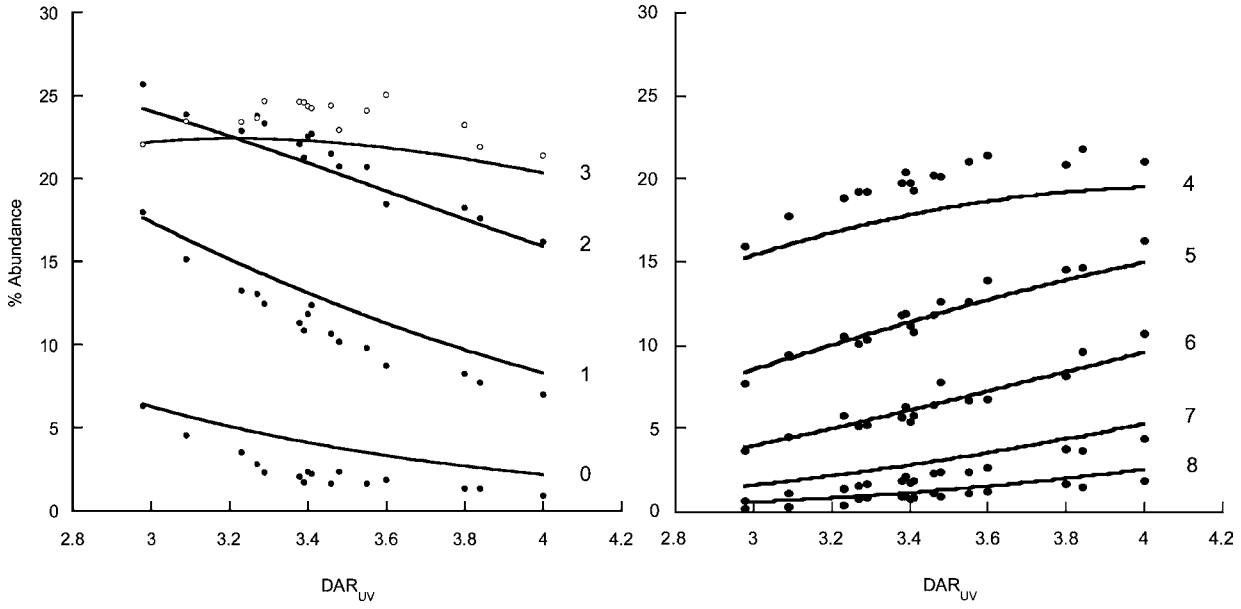

Figure 6. Predicted (solid lines) and experimental (circles) relative abundances of the individual drug load species for all 16 "training" samples. The labels on the right-hand axis indicate the drug load species (0−8). Open circles for drug load 3 species were chosen to avoid confusion between drug load 2 species.

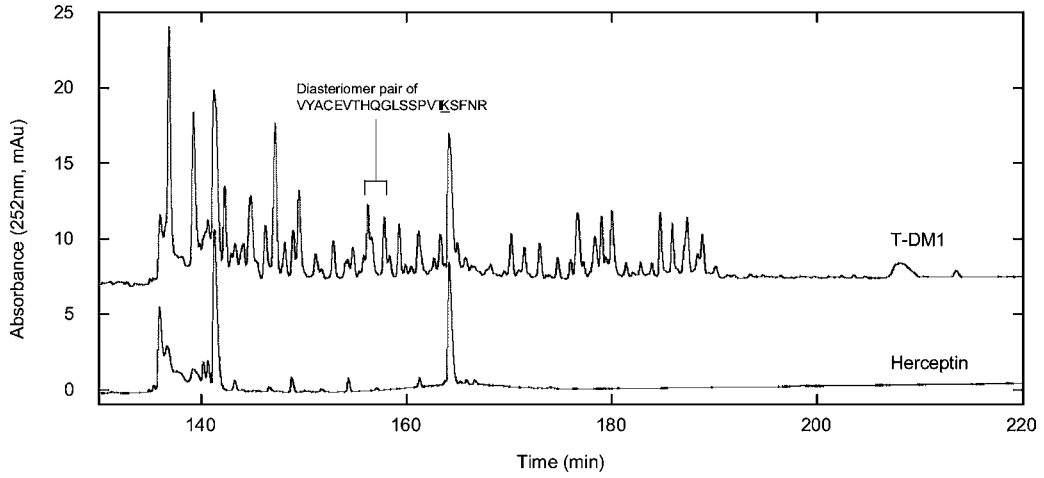

Figure 7. Overlaid UV traces at 252 nm of T-DM1 and Herceptin sample tryptic digests separated by reverse-phase HPLC. An example pair of diasteriomer peaks, corresponding to the same conjugation site, is annotated. Only the portions of each chromatogram showing the elution region of the drug-containing peptides are presented in the figure.

$$B(x) = \frac{17!}{x!(17-x)!} p_{calc}{}^{x}(1-p_{calc})^{17-x} \quad (5b)$$

The same cross-validation procedure described above was then applied to the MS data using the binomial model, generating a maximum error of 2.7%. As with the Poisson model, the largest discrepancies between binomial model and experimental data were from the 0, 1, 3, and 4 drug loads.

Comparison of Poisson and Binomial Models with Known Conjugation Chemistry. Experimental data suggests that conjugation events in trastuzumab emtansine can be characterized as discrete, rare, and independent of one another. The molecular structure of a lysine-linked ADC clearly demonstrates the first characteristic as evidenced by mass-spectrometry. Peptide map analysis supports the remaining two characteristics, rarity and independence. Wang et al. previously described a similar lysine-conjugated molecule, huN901-DM1, and reported over 40 lysines as containing conjugated drug.[14] In our own peptide map analysis of trastuzumab emtansine, approximately 70 sites out of the 88 total lysines and 4 N-terminal amines have been identified as containing attached DM1 using a combination of LC/MS and UV detection at 252 nm which is both sensitive and selective for detecting DM1-conjugated peptides (Figure 7). The large number of sites on trastuzumab that are reactive strongly suggests that the conjugation events are likely to occur independently of each other. Based on the number of sites that could potentially undergo reaction (N = 92) and the average loading level (λ = 3.5), the average site occupancy (p) is predicted to be 3.5/92 or 3.8%, indicating that conjugation is a relatively rare event within the scope of allowable T-DM1 manufacturing conditions (this average site occupancy agrees well with the value calculated by averaging the individual site occupancies, Figure 8).

In agreement with our molecule's conjugation chemistry, the binomial model assumes discrete and independent events.

dx.doi.org/10.1021/bc5000109 | Bioconjugate Chem. 2014, 25, 1223−1232

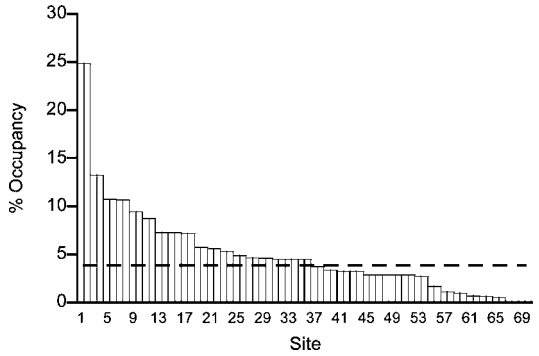

Figure 8. Percent occupancy plotted for all identified conjugatable sites on a typical sample of trastuzumab emtansine, DAR_{UV} = 3.5. Dotted line represents average percent occupancy across all potential conjugation sites (N = 92).

However, the binomial model also requires that the total number of conjugatable lysines and the average probability of a lysine getting conjugated are explicitly specified. The optimized binomial parameters (i.e., those that give the lowest variance and best fit) suggest there are only 17 lysine sites available for conjugation, in direct contradiction to our peptide mapping data which suggests at least 70 conjugatable lysines (Figure 7). As a corollary result, it follows that the suggested average probability of lysine conjugation is overestimated (i.e., for an average drug loading level of 3.5, the suggested average site occupancy is 19% when it is actually closer to ∼4%). Similar qualifying statements about the binomial model were made in a recent study by Skinner et al. The binomial distribution proved useful in deconvoluting mass spectra of their lysine-conjugated antibodies, but Skinner et al. noted that the model parameters did not necessarily represent physically meaningful properties of their conjugation system.[23] In contrast, the Poisson model simply but correctly assumes that the number of available sites is large and discrete and that the lysine conjugation event is rare and independent. While additional optimization of the binomial model is certainly possible (i.e., constraining parameter N to 92) and may lead to comparable results, this is outside the scope of this analysis given that we have already identified a suitable model (the Poisson model) that is straightforward to interpret and that demonstrates the relationship between drug load distribution and average drug load.

The binomial model relative to the Poisson model has a lower maximum error for the current data set (2.7% vs 3.4%) when the value of N was set to 17. However, the Poisson model is simpler in that it requires just one parameter that can be derived experimentally (λ). More importantly, the Poisson model makes valid assumptions regarding our molecule's chemistry, whereas the binomial model suggests specific details regarding the conjugation of trastuzumab emtansine which are misleading (i.e., conjugation occurs at 17 sites, which contradicts our experimentally determined value of ∼70 sites).

Further Tests of Model and Process Robustness. A final set of experiments was performed to test the robustness of the Poisson model and of our process. One key implication of the Poisson model is that—irrespective of the particular process conditions used to generate a sample—T-DM1's drug load distribution should vary only with average DAR. To test the validity of this claim, six samples with similar average DAR (∼3.5) were selected—three from the original model generation data set and an additional three from process development studies that had been prepared using a different selection of process conditions than those included in the DOE experiment detailed in Table 1. Figure 9 shows that despite the differences in process conditions used to make these 6 samples with similar average DAR, there are essentially no differences between their distributions.

Last, we challenged our model by analyzing a sample that was prepared using process conditions significantly displaced from their targets and that resulted in a conjugate with an average DAR of 2.58—well below both the minimal DAR acceptance criterion and the DAR for any of the 16 samples used to train the model. Application of our model to this sample also yielded a predicted drug load distribution that was in excellent

Table 1. T-DM1 Conjugation Processing Conditions and Sample List[a]

	process variable									
	Step 1						Step 2			
sample name	A	B	C	D	E	F	A	B	C	DAR (UV)
1	−1.5%	−4%	−5%	−10%	−3%	−40%	0	0	0	2.98
2	−1.5%	+4%	−5%	+10%	−3%	−40%	0	0	0	3.23
3	+1.5%	+4%	−5%	+10%	+3%	−40%	0	0	0	3.84
4	−1.5%	−4%	+5%	−10%	−3%	+40%	0	0	0	3.09
5	+1.5%	+4%	+5%	+10%	+3%	+40%	0	0	0	4.00
6	0	0	0	0	0	0	0	0	0	3.48
7	0	0	0	0	0	0	−7%	−33%	−25%	3.27
8	0	0	0	0	0	0	−4%	−33%	+25%	3.41
9	0	0	0	0	0	0	+7%	+33%	+25%	3.29
10	0	0	0	0	0	0	−7%	−33%	−25%	3.40
11	0	0	0	0	0	0	−4%	−33%	+25%	3.38
12	0	0	0	0	0	0	0	0	0	3.37
13	0	0	0	0	0	0	0	0	0	3.46
14	0	0	0	0	0	0	−4%	+33%	−25%	3.55
15	0	0	0	0	0	0	+7%	−33%	−25%	3.80
16	0	0	0	0	0	0	−2%	+33%	−25%	3.60

[a]Percentage values indicate differences from target conditions. Target conditions are indicated by the number 0 in all columns, i.e., samples 6, 12, and 13.

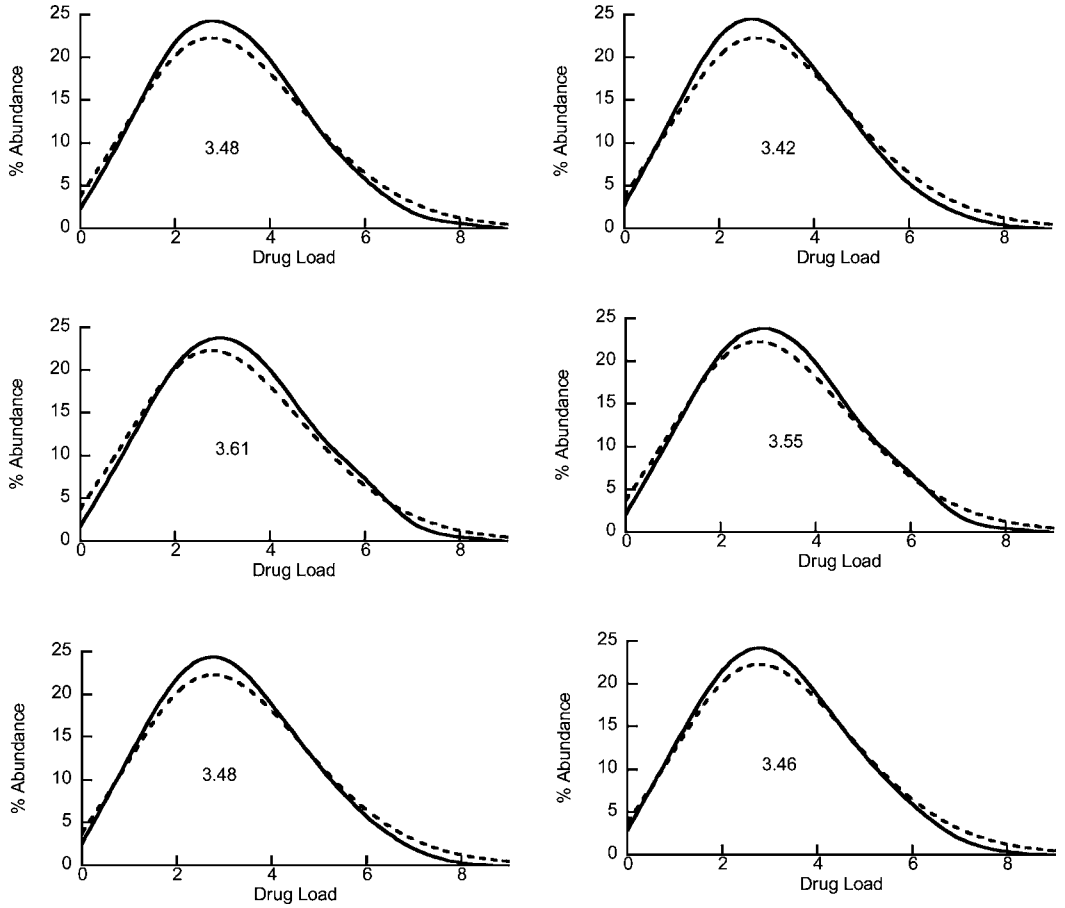

Figure 9. Process robustness data showing that samples generated using different process conditions but with similar average DAR_{UV} (~3.5) have very similar drug load distribution profiles. The number in the center denotes each sample's average DAR_{UV}. Solid lines represent experimental data and the dotted line represents a Poisson predicted drug load distribution for DAR_{UV} = 3.5.

agreement with the experimentally observed distribution (Figure 10). The maximum error between predicted and observed distribution for this sample was 1.7%.

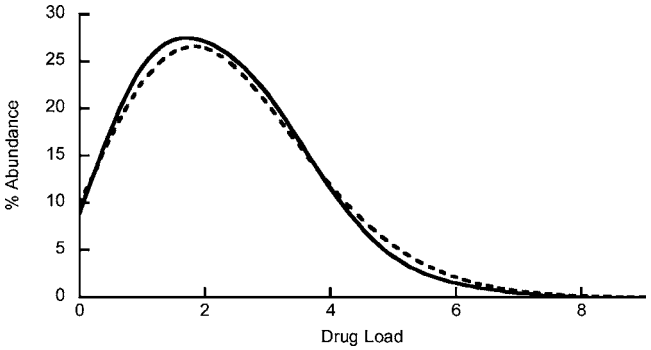

Figure 10. Poisson predicted (dashed) and experimental (solid) drug load distribution profile for a T-DM1 sample with average DAR_{UV} of 2.58.

■ CONCLUSIONS

Chemical conjugation through a protein's lysine residues is well-documented to result in product heterogeneity due to the number and reactivity of the potential target sites.[9,14,21] In the case of a monoclonal antibody, conjugation of drugs using protein amines (lysines and the peptide chain N-termini) results in products with a distribution of drug-loaded forms. Due to the complexity and heterogeneity of these conjugates, no simple chromatographic analytical method that accurately measures the distribution has been developed. Imaged capillary isoelectric focusing (iCIEF) with 280 nm detection is being used to characterize lysine linked conjugates, and the overall distribution of charged species resembles the deconvoluted mass distribution that is observed by MS. However, since the iCIEF peak intensities are significantly influenced by the charged associated variants of the antibody intermediate, the level of cross-linking (if present), and the UV absorbance properties of the drug and/or linker, the data for peaks other than the 0-drug species is difficult to interpret and model. Mass spectrometry can be used to characterize the drug-load distribution; however, this technique would be difficult to move into a quality control laboratory for routine lot-release testing of an ADC for clinical or commercial use. By contrast, UV spectroscopy is a simple and reliable method to determine the average drug to antibody ratio based on the absorbance of the drug and antibody.[6] The purpose of this study was to determine if there is a robust and predictive mathematical relationship between the average DAR and the distribution, which might allow UV spectroscopy to serve as a surrogate test for distribution.

Although some previously published reports have speculated that the distribution of lysine-linked conjugates could be described using the Poisson equation, few details were provided to justify this conclusion. In the work described above, by

dx.doi.org/10.1021/bc5000109 | Bioconjugate Chem. 2014, 25, 1223−1232

applying a statistical analysis to a large enough sample of related molecules, derived from process design-of-experiment studies, the validity of the Poisson model could be verified for trastuzumab emtansine. Different antibodies and conjugation processes are likely to lead to different distributions, so it is not possible yet to predict if this conclusion about the Poisson relation between DAR and distribution can be extended to other lysine-linked ADCs. For example, a recent publication by Boylan et al. demonstrates that for Fc-AF350, a conjugate containing dye molecules attached through lysine residues, a normal distribution is observed over a wide range of DAR (1.5−7.8).[15] Nevertheless, for trastuzumab emtansine, manufactured under well-defined conditions, the drug-load distribution varies as a function of average DAR and can be predicted from that measurement. This implies that the fraction of any specific species (such as the level of unconjugated antibody) can also be derived from the DAR. Therefore, measurement and control of the average DAR using a simple UV spectrophotometric method could be used to indirectly control the drug load distribution for this conjugate. This work is one example of the utility of modeling in the biopharmaceutical industry and helps advocate for further exploration of modeling for ADCs in order to enhance our understanding and our ability to ensure the product quality of these complex therapeutics.

EXPERIMENTAL PROCEDURES

T-DM1 samples for the "training" and "test" data sets were derived from several small-scale multivariate process characterization studies where manufacturing conditions were varied to generate trastuzumab emtansine with a range of DAR values (shown in Table 1). Modification and conjugation are homogeneous solution reactions and the conditions varied include, for example, pH, cosolvent concentrations, reactant stoichiometries, reaction times, buffer, and other solute concentrations and temperature. The target conditions for the reaction are indicated by the number 0 in Table 1, while the extent of the variation evaluated in the experimental design is indicated by the $\pm x$%. Assignment of samples to the "training" set or "test" data set as part of the hold-out cross-validation analysis will be described below.

Average DAR by UV/vis Absorbance Spectroscopy. UV spectroscopy was used to simultaneously determine the concentrations of antibody and drug.[6,15] Two of the components of T-DM1, trastuzumab antibody and DM1 drug, absorb strongly at 280 and 252 nm, respectively, and contribute to the resulting UV spectrum of the antibody−drug conjugate (Figure 4). The MCC linker does not have significant absorbance at either of these wavelengths. Based on the extinction coefficients of each component at these wavelengths ($\varepsilon_{280\ \mathrm{DM1}}$ = 5700 M^{-1} cm^{-1}, $\varepsilon_{252\ \mathrm{DM1}}$ = 26 790 $M^{-1}cm^{-1}$ and $\varepsilon_{280\ \mathrm{Tmab}}$ = 218 134 $M^{-1}cm^{-1}$, $\varepsilon_{252\ \mathrm{Tmab}}$ = 76 565 $M^{-1}cm^{-1}$), the solution of a pair of simultaneous linear equations allows calculation of the molar concentrations of antibody and of DM1 from the measured absorbances at 280 and 252 nm. The average DAR (expressed as moles of DM1 per mole of antibody) is then derived from the ratio of the DM1 and antibody concentrations. Spectra were taken using a dual-beam UV/vis spectrophotometer (PerkinElmer Lambda 25) of samples diluted to approximately 0.5 mg/mL in formulation buffer. The instrument was blanked against the same buffer and measurements were performed at ambient temperature.

Experimentally Determined Drug Load Distribution Using Intact LC-MS. MS analysis of intact and deglycosylated T-DM1 was performed using a PE-Sciex QSTAR Pulsar mass spectrometer. Protein was deglycosylated by incubation overnight at pH 7.5 in 100 mM Tris buffer at 37 °C in the presence of PNGase F (New England Biolabs) at a ratio of 5000 units per mg antibody. Samples (20 μg) were introduced into the mass spectrometer using an RP-HPLC column (Agilent POROSHELL 300SB, C8, 1.0 × 75 mm, 5 μm, 300 Å) run at 0.2 mL/min and equilibrated at 75 °C with 82% solvent A (0.1% formic acid in water). After equilibration with 82% solvent A for 10 min, samples were eluted using a 16 min linear gradient from 18% to 95% solvent B (0.1% formic acid in acetonitrile). The capillary and cone voltages of the mass spectrometer were optimized for maximum sensitivity. The final instrument conditions included an electrospray voltage of 5200 V, a first declustering potential (DP1) of 60 V, a second declustering potential (DP2) of 15 V, a focusing potential of 200 V, and a capillary temperature of 350 °C. Mass spectra were derived by deconvolution of the multiply charged ions using Analyst QS 1.1 software. Integration of the resulting peaks was performed using the same software package. As seen in Figure 2, the mass spectrum exhibits a minor, secondary distribution with masses ∼220 Da higher than the primary set of peaks. Each of these corresponds to a drug loaded species that also contains an MCC linker that has reacted to form an internal cross-link. The sum of the peak areas (for the drug-loaded species and the corresponding species with the extra linker) is used to calculate the percent peak area associated with each drug-load level.

Identification and Percent Occupancy Determination of Each Conjugation Site Using LC-MS/MS. Tryptic peptide map analysis, in conjunction with high-resolution liquid chromatography-tandem mass spectrometry, was performed on a representative sample of trastuzumab emtansine (DAR: 3.5) and a sample of unconjugated trastuzumab (Herceptin) to identify the conjugated lysine sites and calculate percent occupancy at each available site. Reduction and S-carboxymethylation of cysteines was performed prior to digestion with trypsin. Samples containing 1 mg (50 μL) of trastuzumab emtansine or trastuzumab were diluted to 1 mg/mL into a pH 8.6 buffer containing 6 M guanidine hydrochloride, 0.36 M Tris-HCl, and 2 mM EDTA. DTT (Thermo Scientific) was added to bring the samples to 10 mM, and the samples were then incubated at 37 °C for 1 h. Iodoacetic acid (Sigma), freshly prepared in 1.0 M sodium hydroxide, was then added to a concentration of 42 mM. After a 20 min incubation at ambient temperature in the dark, the alkylation was quenched by adding DTT to a final concentration of 40 mM. The reduced and S-carboxymethylated sample was then exchanged by gel filtration using PD-10 columns (GE Healthcare) into a pH 8.3 buffer containing 25 mM Tris-HCl and 1 mM calcium chloride. Trypsin (Sequencing grade, Roche) was added to the samples at a 1:40 (w/w) ratio. Digestion was allowed to proceed for 4 h at 37 °C, and then quenched by addition of TFA to bring the samples to 0.5% TFA (v/v). Digested samples (100 uL, approximately 50 ug) were analyzed by RP-HPLC on a Zorbax 300SB-C8 column (2.1 × 150 mm, 3.5 μm particle) equilibrated with 100% solvent A (0.1% TFA in water) using an Agilent 1200 HPLC system. The column was eluted at a flow rate of 0.25 mL/min and maintained at 45 °C. Peptides were resolved with a linear gradient from 0% to 45% solvent B

Table 2. T-DM1 Conjugation Processing Conditions of Four Additional Samples[a]

	process variables									
	step 1						step 2			
sample name	A	B	C	D	E	F	A	B	C	DAR (UV)
1	+1.5%	+4%	−5%	−10%	−3%	+40%	0	0	0	3.48
2	−1.5%	+4%	+5%	−10%	+3%	−40%	0	0	0	3.42
3	+1.5%	−4%	+5%	+10%	−3%	−40%	0	0	0	3.55
4	0	0	0	0	−26%	0	0	0	0	2.58

[a]Percentage values indicate differences from target conditions.

(0.09% TFA in acetonitrile) over 225 min. The chromatogram was developed with a multistep gradient as follows: 0−45% solvent B in 225 min, 45−95% solvent B in 5 min, equilibration at 95% solvent B for 5 min, and back to 0% solvent B in 0.1 min with equilibration at 0% for 14.9 min. Absorbance was monitored at both 214 and 252 nm and column flow was directed into the source of an LTQ or a QSTAR Pulsar mass spectrometer. Data were analyzed using XCalibur 2.0.7, Analyst QS 1.1 and MASCOT search engine. As seen in Figure 7, each conjugated peptide elutes as two new peaks because of the two stereochemical configurations (diastereomers) of the antibody−drug linkage through a maleimide. The conjugation levels at each site were quantified by determining both the drop in the starting peptide UV peak area (at 214 nm) and the increase of new drug-containing peptide UV peak areas (252 nm) between trastuzumab and trastuzumab emtansine samples.

Additional Process and Model Robustness Studies. An additional four samples were analyzed which were not included in the original model generation and cross-validation data set for further evaluation of distribution and agreement with the model. Three of the samples had average DAR values of ∼3.5 and were selected from the process characterization study. These samples had been produced using different process parameters to test robustness of the conjugate manufacturing (shown in Table 2). Next, the process was run under conditions far removed from their targeted set-points to produce the fourth and final sample with DAR 2.58 (Table 2). This sample was also analyzed by mass spectrometry and its distribution was fit to the same model.

COMPUTATIONAL METHODS

Screening of Discrete Models for Predicting Drug Load Distributions. General forms of the Poisson, geometric, negative binomial, binomial, and hypergeometric equations were explored as potential models for predicting drug load distribution from the average DAR. Parameters for each model were numerically optimized using the iterative Gauss−Newton algorithm to fit the drug load distributions from the sample set (containing 16 trastuzumab emtansine samples selected from the process characterization study with average DAR values ranging from 3.0 to 4.0), minimizing the total variation distance. The high and low limits of DAR represented in the set extend beyond the acceptance criterion of this attribute for use in the clinic. The models with the best fit were selected for further analysis.

Cross-Validation. To assess the accuracy of the selected model, a hold-out cross validation was performed. The test samples are partitioned into disjoint "training" (13 of the 16 samples) and "test" (using the held-out remaining 3) sets of data. During each iteration, the model is fit to the "training" set and then evaluated using the "test" set of data. After all the possible permutations of "training" set−"test" set pairings were evaluated (560 combinations), an aggregated error statistic was generated from the cross-validation procedure.

AUTHOR INFORMATION

Corresponding Author

*E-mail: michaetk@gene.com.

Notes

The authors declare the following competing financial interest(s): Authors are employees of Hoffmann-La Roche Inc.

ACKNOWLEDGMENTS

The authors would like to thank Laura Zheng for her help with LC/MS and Pat Rancatore for her insightful comments and review.

ABBREVIATIONS

ADC, antibody−drug conjugate; DM1, *N*2′-deacetyl-*N*2′-(3-mercapto-1-oxopropyl)-maytansine; SMCC, succinimidyl-4-(*N*-maleimidomethyl)cyclohexane-1-carboxylate; DAR, drug to antibody ratio; T-DM1, trastuzumab emtansine

REFERENCES

(1) Chari, R. V. J. (2008) Targeted cancer therapy: conferring specificity to cytotoxic drugs. *Acc. Chem. Res. 41*, 98−107.

(2) Wu, A. M., and Senter, P. D. (2005) Arming antibodies: prospects and challenges for immunoconjugates. *Nat. Biotechnol. 23*, 1137−1146.

(3) DiJoseph, J. F., Dougher, M. M., Armellino, D. C., Evans, D. Y., and Damle, N. K. (2007) Therapeutic potential of CD22-specific antibody-targeted chemotherapy using inotuzumab ozogamicin (CMC-544) for the treatment of acute lymphoblastic leukemia. *Leukemia 21*, 2240−2245.

(4) Phillips, G. D. L., Li, G., Dugger, D. L., Crocker, L. M., Parsons, K. L., Mai, E., Blattler, W. A., Lambert, J. M., Chari, R. V. J., Lutz, R. J., Wong, W. L. T., Jacobson, F. S., Koeppen, H., Schwall, R. H., Kenkare-Mitra, S. R., Spencer, S. D., and Sliwkowski, M. X. (2008) Targeting HER2-positive breast cancer with Trastuzumab-DM1, an antibody-cytotoxic drug conjugate. *Cancer Res. 68*, 9280−9290.

(5) Younes, A., Bartlett, N. L., Leonard, J. P., Kennedy, D. A., Lynch, C. M., and Sievers, E. L. (2010) Brentuximab vedotin (SGN-35) for relapsed CD30-positive lymphomas. *New Engl. J. Med. 363*, 1812−1821.

(6) Wakankar, A., Chen, Y., Gokarn, Y., and Jacobson, F. S. (2011) Analytical methods for physicochemical characterization of antibody drug conjugates. *mAbs 3*, 161−172.

(7) Junutula, J. R., Raab, H., Clark, S., Bhakta, S., Leipold, D. D., Weir, S., Chen, Y., Simpson, M., Tsai, S. P., Dennis, M. S., Lu, Y., Meng, Y. G., Ng, C., Yang, J., Lee, C. C., Duenas, E., Gorrell, J., Katta, V., Kim, A., McDorman, K., Flagella, K., Venook, R., Ross, S., Spencer, S. D., Wong, W. L., Lowman, H. B., Vandlen, R., Sliwkowski, M. X., Scheller, R. H., Polakis, P., and Mallet, W. (2008) Site-specific conjugation of a cytotoxic drug to an antibody improves the therapeutic index. *Nat. Biotechnol. 26*, 925−932.

(8) Hamann, P. R., Hinman, L. M., Hollander, I., Beyer, C. F., Lindh, D., Holcomb, R., Hallett, W., Tsou, H.-R., Upeslacis, J., Shochat, D., Mountain, A., Flowers, D. A., and Bernstein, I. (2002) Gemtuzumab Ozogamicin, a potent and selective anti-CD33 antibody-Calicheamicin conjugate for treatment of acute myeloid leukemia. *Bioconjugate Chem. 13*, 47−58.
(9) Lu, S. X., Takach, E. J., Solomon, M., Zhu, Q., Law, S.-j., and Hsieh, F. Y. (2004) Mass spectral analyses of labile DOTA-NHS and heterogeneity determination of DOTA or DM1 conjugated anti-PSMA antibody for prostate cancer therapy. *J. Pharm. Sci. 94*, 788−797.
(10) Siegel, M. M., Tabei, K., Kunz, A., Hollander, I. J., Hamann, P. R., and Bell, D. H. (1997) Calicheamicin derivatives conjugated to monoclonal antibodies: Determination of loading values and distributions by Infrared and UV matrix-assisted laser desorption/ionization mass spectrometry and electrospray ionization mass spectrometry. *Anal. Chem. 69*, 2716−2726.
(11) Stephan, J.-P., Chan, P., Lee, C., Nelson, C., Elliott, J. M., Bechtel, C., Raab, H., Xie, D., Akutagawa, J., Baudys, J., Saad, O., Prabhu, S., Wong, W. L. T., Vandlen, R., Jacobson, F., and Ebens, A. (2008) Anti-CD22-MCC-DM1 and MC-MMAF conjugates: impact of assay format on pharmacokinetic parameters determination. *Bioconjugate Chem. 19*, 1673−1683.
(12) Sun, M. M. C., Beam, K. S., Cerveny, C. G., Hamblett, K. J., Blackmore, R. S., Torgov, M. Y., Handley, F. G. M., Ihle, N. C., Senter, P. D., and Alley, S. C. (2005) Reduction-alkylation strategies for the modification of specific monoclonal antibody disulfides. *Bioconjugate Chem. 16*, 1282−1290.
(13) Hamblett, K. J., Senter, P. D., Chace, D. F., Sun, M. M. C., Lenox, J., Cerveny, C. G., Kissler, K. M., Bernhardt, S. X., Kopcha, A. K., Zabinski, R. F., Meyer, D. L., and Francisco, J. A. (2004) Effects of drug loading on the antitumor activity of a monoclonal antibody drug conjugate. *Clin. Cancer Res. 10*, 7063−7070.
(14) Wang, L., Amphlett, G., Blattler, W. A., Lambert, J. M., and Zhang, W. (2005) Structural characterization of the maytansinoid-monoclonal antibody immunoconjugate, huN901-DM1, by mass spectrometry. *Protein Sci. 14*, 2436−2446.
(15) Boylan, N. J., Zhou, W., Proos, R. J., Tolbert, T. J., Wolfe, J. L., and Laurence, J. S. (2013) Conjugation site heterogeneity causes variable electrostatic properties in Fc conjugates. *Bioconjugate Chem. 24*, 1008−1016.
(16) Kunz, A., Moran, J., Rubino, J., Jain, N., Vidunas, E., Simpson, E., Robbins, P., Merchant, N., DiJoseph, J., Ruppen, M., Damle, N., and Popplewell, A. Calicheamicin derivative-carrier conjugates, U.S. Patent 8,153,768, April, 10, 2012.
(17) Wakankar, A. A., Feeney, M. B., Rivera, J., Chen, Y., Kim, M., Sharma, V. K., and Wang, Y. J. (2010) Physicochemical stability of the antibody-drug conjugate Trastuzumab-DM1: Changes due to modification and conjugation processes. *Bioconjugate Chem. 21*, 1588−1595.
(18) Dent, A. H. (2007) Optimizing bioconjugation processes. *Pharmceutical Technology Europe 19*, 39.
(19) Sako, Y., Minoguchi, S., and Yanagida, T. (2000) Single-molecule imaging of EGFR signalling on the surface of living cells. *Nat. Cell Biol. 2*, 168−172.
(20) Vira, S., Mekhedov, E., Humphrey, G., and Blank, P. S. (2010) Fluorescent-labeled antibodies: Balancing functionality and degree of labeling. *Anal. Biochem. 402*, 146−150.
(21) Lazar, A. C., Wang, L., Blattler, W. A., Amphlett, G., Lambert, J. M., and Zhang, W. (2005) Analysis of the composition of immunoconjugates using size-exclusion chromatography coupled to mass spectrometry. *Rapid Commun. Mass Spectrom. 19*, 1806−1814.
(22) Hawe, A., Sutter, M., and Jiskoot, W. (2008) Extrinsic fluorescent dyes as tools for protein characterization. *Pharm. Res. 25*, 1487−1499.
(23) Skinner, J. P., Chi, L., Ozeata, P. F., Ramsay, C. S., O'Hara, R. L., Calfin, B. B., and Tetin, S. Y. (2012) Introduction of the mass spread function for characterization of protein conjugates. *Anal. Chem. 84*, 1172−1177.